Chameleon Field Theories and Fifth Force

Alton Vanie Kesselly (vanie@aims.ac.za)
African Institute for Mathematical Sciences (AIMS)

Supervised by: Doctor Amanda Weltman
University of Cape Town, South Africa

23 May 2013

Submitted in partial fulfillment of a structured masters degree at AIMS South Africa

Abstract

Despite its elegance, simplicity, aestheticism and its empirical successes in the laboratory and on solar system scales, the failure to harmonize Einstein's theory of general relativity with Quantum physics and the inability to use it to explain the current acceleration of the universe suggest that it is, at best, an effective theory. Attempts at making it into a complete theory of gravity usually leads to inconsistencies with tests of gravity. For instance, the addition of the cosmological constant to Einstein's field equations allows them to adequately account for the current acceleration of the universe but with the unsettling issues of fine-tuning and cosmic coincidence. A way of alleviating these problems, particularly the cosmic coincidence problem, is by attributing the acceleration of the universe to dark energy and then generalizing the dark energy as scalar fields slowly rolling down a flat potential. But, doing so introduces a new force of nature, the so-called fifth force, which leads to inconsistencies with local tests of gravity.

Chameleon fields provide the mechanisms that suppress the magnitude of the fifth force, making it to fit within the confines of current empirical constraints. In regions of high density, the chameleon becomes short-ranged to satisfy current constraints and for a sufficiently large object the fifth force is due almost entirely to only a thin-shell just beneath the surface of the large object.

Keywords: Chameleon, Fifth force, thin-shell, thick-shell, Equivalence Principle, Conformal coupling, Quintessence

Declaration

I, the undersigned, hereby declare that the work contained in this essay is my original work, and that any work done by others or by myself previously has been acknowledged and referenced accordingly.

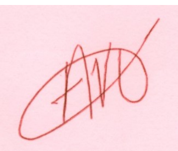

Alton Vanie Kesselly, 23 May 2013

Contents

1. Introduction

1.1 Outlook

Firm and stout as Einstein's theory of gravitation seems, its incompatibility with grand unification schemes of Physics (in addition to its inability to adequately explain recent observations like the acceleration of the universe) makes the need for its modification a must. Yet, most attempts at modifying Einstein's theory of gravitation (i.e., String Theory, Supergravity and quintessence) point to the problematic existence of additional fields, including scalar fields, that can couple to matter fields or the metric. On one hand, the coupling of these scalar fields to matter or the metric is a curse in that such coupling leads to variation of fundamental constants and to the introduction of a fifth force which do not fit within the bounds of current empirical constraints. On the other hand, it is a blessing in that such coupling makes it possible to generalize dark energy as scalar fields slowly rolling down a flat potential and thus alleviating some of the theoretical problems associated with explaining the current acceleration of the universe.

The Chameleon mechanism is a way out of this predicament. The Chameleon comes with two distinct features that allow scalar fields to couple with matter fields or the metric and yet remain compatible with observations.

This essay reviews these unique characteristics of the chameleon. In this chapter, we introduce Einstein's theory of gravitation. We also introduce Cosmology and scalar field theories. This chapter is intended to introduce the basic equations, concepts and to maintain the narrative needed for easy reading of subsequent chapters of this essay. It is also intended to set the basis for ensuing arguments. In Chapter 2, the equations of motion of chameleon field theories are derived via the action principle and in so doing we get, as by-product, one of the unique features of the chameleon. These equations of motion are then solved for both compact bodies and vacuum chambers and we get, for free, the other distinct feature of the chameleon. The claim that a fifth force can exist and yet be hidden by chameleonic effect is subjected to the stringent of tests and proved probable in chapter 3. There, we also review how to go out detecting the fifth force and we examine the bold prediction made by the progenitors of the Chameleon model. Chapter 4 summaries the entire essay and concludes with personal perspectives and suggestions.

1.2 Einsten's Theory of General Relativity

Newton's law of universal gravity is wanting as a modern theory of gravitation. For instance, it is not Lorentz invariant. Desire of overhauling it led to the creation of Einstein's theory of General Relativity. The centrepiece of Einstein's theory of general relativity is Einstein's field equations,

$$G_{\mu\nu} = R_{\mu\nu} - \frac{1}{2} R g_{\mu\nu} = 8\pi T_{\mu\nu}. \tag{1.2.1}$$

Some of the the most important terms associated with Einstein's theory of General relativity are defined mathematically as follows:[1]

the Riemann tensor

$$R^{\rho}_{\sigma\mu\nu} = \partial_\mu \Gamma^{\rho}_{\nu\sigma} - \partial_\nu \Gamma^{\rho}_{\mu\sigma} + \Gamma^{\rho}_{\mu\lambda}\Gamma^{\lambda}_{\nu\sigma} - \Gamma^{\rho}_{\nu\lambda}\Gamma^{\lambda}_{\mu\sigma}, \tag{1.2.2}$$

[1] Unless otherwise stated, all the subsequent equations and mathematical definitions are taken from (Carroll, 2004)

the Ricci tensor

$$R_{\mu\nu} = R^{\lambda}_{\sigma\lambda\nu}, \tag{1.2.3}$$

the Ricci scalar

$$R = R^{\mu}_{\mu} = g^{\mu\nu} R_{\mu\nu}, \tag{1.2.4}$$

the energy-momentum tensor for a perfect fluid[2]

$$T_{\mu\nu} = \Big(\rho + p\Big) u_\mu u_\nu + p g_{\mu\nu}, \tag{1.2.5}$$

the connection or Christoffel symbols

$$\Gamma^{\rho}_{\mu\nu} = \frac{1}{2} g^{\lambda\sigma}\Big(\partial_\mu g_{\nu\sigma} + \partial_\nu g_{\sigma\mu} - \partial_\sigma g_{\mu\nu}\Big), \tag{1.2.6}$$

geodesics for a particle with worldline x^μ

$$\frac{d^2 x^\mu}{d\lambda^2} = \Gamma^{\mu}_{\rho\sigma} \frac{dx^\rho}{d\lambda}\frac{dx^\sigma}{d\lambda} = 0, \tag{1.2.7}$$

and $u^\rho = \dfrac{dx^\rho}{d\lambda}$ is a 4-velocity,

d'Alembertian operator

$$\Box = \nabla^\mu \nabla_\mu = g^{\mu\nu}\nabla_\mu \nabla_\nu = -\partial_t^2 + \nabla^2, \tag{1.2.8}$$

which for a static field becomes

$$\Box = \nabla^\mu \nabla_\mu = \nabla^2, \tag{1.2.9}$$

an invariance for timelike spacetime

$$g_{\mu\nu}\frac{dx^\mu}{d\lambda}\frac{dx^\nu}{d\lambda} = g_{\mu\nu} u^\mu u^\nu = u^\mu u_\nu = -1, \tag{1.2.10}$$

a Covariant derivative for a contravariant 4-vector, V^μ

$$\nabla_\mu V^\nu = \partial_\mu V^\nu + \Gamma^{\nu}_{\mu\sigma} V^\sigma, \tag{1.2.11}$$

a Covariant derivative for a covariant 4-vector, w_ν

$$\nabla_\mu w_\nu = \partial_\mu w_\nu - \Gamma^{\lambda}_{\mu\nu} V_\lambda, \tag{1.2.12}$$

The cornerstone of Einstein's theory of general relativity is the so-called Equivalence Principle (EP). The Equivalence Principle implies, among other things, that local gravitational effects can be eliminated by a suitable choice of reference frame. This is epitomized by the popular quote: "a person falling freely in a gravitational field doesn't feel her own weight."[3] In other words, gravitational interaction can be identified with geometry. The Equivalence Principle can be stated more formally as: all test bodies fall with the same acceleration regardless of their internal structure and composition and the results of localized non-gravitational experiments are independent of the velocity of the frame they are performed in (Local Lorentz invariance) and are also independent of when and where in the universe they were performed (Local Position Invariance)(Will, 2005) (Camenzind, 2007).

[2]The energy-momentum tensor used in Cosmology is assumed to be a perfect fluid

[3]Einstein considered this statement as the happiest thought of his life.

The Equivalence Principle (actually, the weak Equivalence Principle) assumes that the inertial mass and the passive gravitational mass are equal:[4]

$$M_I = M_P. \tag{1.2.13}$$

Yet, the inertial mass is made up of different types of mass-energy, including rest mass, electromagnetic energy, chemical energy, weak interaction energy, etc., and there is no a-priori reason why each of these different forms of energy should contribute equally to both M_I and M_P. So, one way that the equivalence Principle can be violated is for any one of these forms of energy to contribute differently to M_I than it does to M_P. Such violations are usually written as:

$$M_P = M_I + \sum_A \eta_A \frac{E^A}{c^2}. \tag{1.2.14}$$

E^A denotes the internal energy of the body generated via the interaction A. η_A,called E$\ddot{o}$tvos ratio, is a dimensionless parameter that quantifies the violation of the Equivalence Principle induced by interaction A. That is, it is the measurement or limit on the difference between the accelerations of two test bodies, say a_1 and a_2 and is defined mathematically as:

$$\eta = 2\left|\frac{a_1 - a_2}{a_1 + a_2}\right| = \sum_A \eta^A \left(\frac{E_1^A}{M_{I,1}c^2} - \frac{E_2^A}{M_{I,2}c^2}\right) \tag{1.2.15}$$

The best limit on test of the Equivalence Principle, $\eta < 10^{-13}$, comes from the Eot-Wash experiment and the Lunar Laser Ranging (LLR) experiment (Will, 2005) but with the launch of the Satellites Test of the Equivalence Principle (STEP), MICROSCOPE and Galileo Galilei(GG) (Khoury and Weltman, 2004a) (Nobili et al., 2009),(Dittus and Lämmerzahl, 2005) tests for violation of the Equivalence Principle are expected to reach to sensitivity as high as 10^{-18}.

Despite be subjected to the the most stringent of tests, there is yet no violation of the Equivalence principle. Thus, violation of the Equivalence principle now passes as some sort of gold standard test for all theories of gravity that intend supplanting Einstein's theory of general relativity as the de facto theory of gravitation.

The Bianchi's identity

$$\nabla^\mu G_{\mu\nu} = 0, \tag{1.2.16}$$

which is synonymous with the cherished principle of energy conservation

$$\nabla^\mu T_{\mu\nu} = 0, \tag{1.2.17}$$

means that the Einstein's field equations are not unique. They can be modified in order to extend their usefulness into forbidden territories-arenas where they were once deemed not valid. One way of doing so, which Einstein himself did, is the addition of the so-called Cosmological constant, Λ, to Einstein's field equations. With the addition of the Cosmological constant, Einstein's field equations becomes:

$$G_{\mu\nu} = R_{\mu\nu} - \frac{1}{2}Rg_{\mu\nu} + \Lambda g_{\mu\nu} = 8\pi T_{\mu\nu}. \tag{1.2.18}$$

By the way, the addition of a cosmological constant to Einstein's field equations was actually done out of the necessity to have these equations describe a static universe.[5]

[4]this discussion on the EP and accompanying equations are either patterned after or taken directly from (Camenzind, 2007) and (Will, 2005)

[5] When Hubble showed that the universe was expanding, Einstein immediately withdrew the Cosmological constant with the remark that the introduction of the cosmological constant was the greatest blunder of his life. Since Einstein, the cosmological constant has been discarded numerous times but like the proverbial Phoenix it keeps arising over and again. See (Weinberg, 1989),(Carroll et al., 1992)(Padmanabhan, 2003) for details.

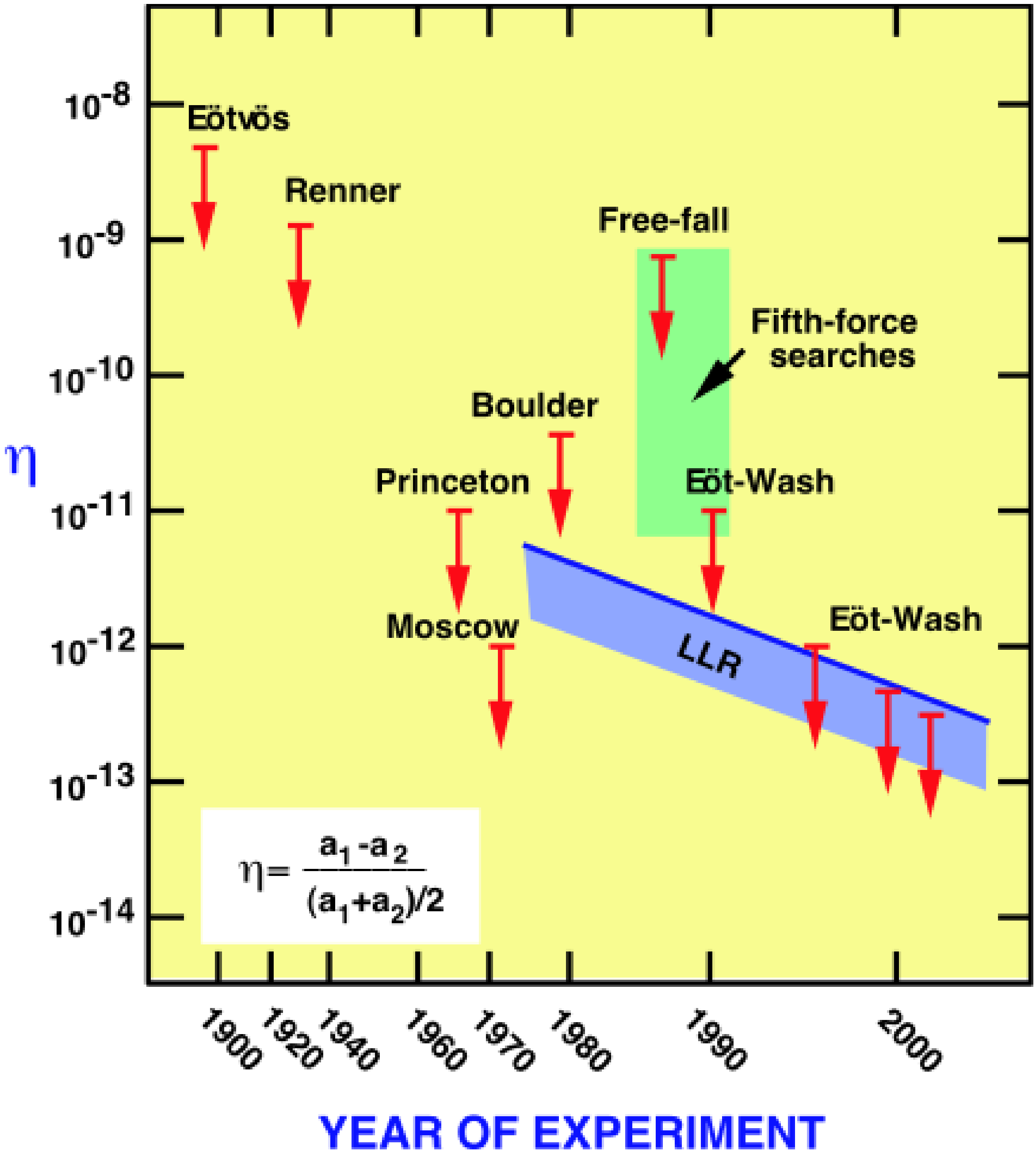

Figure 1.1: Results of selected test on EP showing the bounds on η. Courtesy of: (Will, 2005)

1.3 Cosmology

Cosmology, the study of the origin, fate, structure and composition of the universe hinged on the premise-the Cosmological Principle- that we don't live in a special place (or time) in the universe. This implies that on large scale (about 100 Mpc) the universe is spatially homogeneous and isotropic but evolves with time (Blau, 2011).

The metric that is compatible with the cosmological principle, the Friedmann-Robertson-Walker metric (FRW), can be written as:

$$ds^2 = dt^2 - a^2(t)\Big(\frac{dr^2}{\sqrt{1-kr^2}} + r^2(d\theta^2 + sin^2\theta d\phi^2\Big). \tag{1.3.1}$$

ϕ and θ are the usual azimuthal and polar angles of the spherical coordinates with ranges $0 \leq \phi \leq 2\pi$ and $0 \leq \theta \leq \pi$, the parameter k can be either 0 (for a flat universe), 1 (closed universe) or -1 (open universe) and $a(t)$ is the cosmic expansion factor.

Using the FRW metric equation (1.3.1) in Einstein's field equation (1.2.1) results in the Friedmann equations,

$$\frac{\dot{a}^2}{a^2} = \frac{8\pi G\rho}{3} - \frac{k}{a^2} \tag{1.3.2}$$

$$\frac{\ddot{a}}{a} = -\frac{4\pi G}{3}(\rho + p). \tag{1.3.3}$$

The evolution of the universe is conventionally quantified by the Hubble parameter, H which can be defined as:

$$H \equiv \frac{\dot{a}}{a}. \tag{1.3.4}$$

The density required to make the universe flat, called the critical density, is

$$\rho_{crit} \equiv \frac{3H^2}{8\pi G}. \tag{1.3.5}$$

The ratio of the actual density of the universe ρ to the critical density, symbolized by the Ω, is,

$$\Omega \equiv \frac{\rho}{\rho_{crit}}. \tag{1.3.6}$$

The different components that contribute to the density of the universe are radiations (i.e., photons and neutrino), ρ_γ, matter (ordinary matter and baryonic and non-baryonic dark matter) ρ_m and Dark energy ρ_Λ. At different epochs, one of them dominates the total density of the universe and it thus dictates the evolutionary behaviours of the universe during that particular epoch.

The equation of state that relates the density ρ to the pressure p of the fluid, that is described by the energy-momentum tensor of a perfect fluid (1.2.5), is given by

$$w = \frac{p}{\rho}. \tag{1.3.7}$$

$w = 0$ for matter, $\frac{1}{3}$ for radiation and -1 for dark energy[6]. Depending on the value of w, the expansion of the universe could be either slowing down or picking up speed. In fact, there are now

[6] actually the version of dark energy called vacuum energy

overwhelming evidence that the expansion of the universe is actually speeding up (Riess et al., 1998)(Frieman et al., 2008).

Though the Cosmological constant perfectly fits the bill for the acceleration of the universe, it comes with two nettlesome baggages that theorists find very unsettling. These two nuisances are dubbed the Fine-tuning problem and the Coincidence problem. Theorists just can not fathom why the density of the cosmological constant is so small yet non-zero (fine-tuning) and they are bewildered at how the ratio of the density of matter to the density of dark matter that was of an order of10^{100}, ($\frac{\rho_m}{\rho_\Lambda} \sim 10^{100}$) in the early universe became an order unity, $\frac{\rho_m}{\rho_\Lambda} \sim 0(1)$ just at the time intelligent beings appear to observe it (Coincidence problem)(Carroll et al., 1992).

A possible escape hatch for this theoretical purgatory is the invocation of the concept of quintessence (Zlatev et al., 1999)(Carroll, 1998). That is, generalizing the dark energy as a scalar field rolling down a flat potential. With this, the values of w now ranges between -1 and $-\frac{1}{3}$ or

$$-1 \leq w \leq -\frac{1}{3}. \tag{1.3.8}$$

1.4 Scalar Fields

Another way of modifying Einstein's field Equations is by adding scalar fields. An illuminating and instructive way of doing this is via the action principle and also through conformal coupling of the scalar to the metric or to matter. That is, introducing an action of the form[7]

$$S_\phi = \int d^4x \mathcal{L}(\phi^i, \nabla_\mu \phi^i) \tag{1.4.1}$$

and by directly coupling the scalar to the metric via

$$\tilde{g}_{\mu\nu} = f^2(\phi) g_{\mu\nu}. \tag{1.4.2}$$

f is a function of ϕ, the metric with tilde belong to Jordan frame and those without tilde belong to Einstein frame.

Varying the action with respect to the fields gives the equations of motion of the fields

$$\frac{\delta S}{\delta \phi^i} = \frac{\partial \mathcal{L}}{\partial \phi^i} - \partial_\mu \left(\frac{\partial \mathcal{L}}{\partial(\partial_\mu \phi^i)} \right) = 0 \tag{1.4.3}$$

whereas varying the action with respect to the metric gives the energy-momentum tensor of the fields

$$T_{\mu\nu} = -2 \frac{1}{\sqrt{-g}} \frac{\delta S_m}{\delta g^{\mu\nu}}. \tag{1.4.4}$$

In the Jordan's frame, Equation (1.2.6) becomes:

$$\tilde{\Gamma}^\rho_{\mu\nu} = \frac{1}{2} g^{\tilde{\lambda}\sigma} \Big(\partial_\mu \tilde{g}_{\nu\sigma} + \partial_\nu \tilde{g}_{\sigma\mu} - \partial_\sigma \tilde{g}_{\mu\nu} \Big). \tag{1.4.5}$$

[7]Again, these equations are patterned after those of (Carroll, 2004)

Substituting Equation (1.4.2) into Equation (1.4.5) leads to

$$\tilde{\Gamma}^{\rho}_{\mu\nu} = \Gamma^{\rho}_{\mu\nu} + f^{-1}\Big(\delta^{\rho}_{\mu}\nabla_{\nu}f + \delta^{\rho}_{\nu}\nabla_{\mu}f - g_{\mu\nu}g^{\rho\lambda}\nabla_{\lambda}f\Big). \tag{1.4.6}$$

$$\frac{d^2x^{\mu}}{d\lambda^2} + \tilde{\Gamma}^{\mu}_{\rho\sigma}\frac{dx^{\rho}}{d\lambda}\frac{dx^{\sigma}}{d\lambda} = 0 \tag{1.4.7}$$

is the geodesics for particle with worldline x^{μ} in the Jordan's frame.

(1.4.6) into (1.4.7) gives:

$$\frac{d^2x^{\mu}}{d\lambda^2} + \Gamma^{\rho}_{\mu\nu}\frac{dx^{\rho}}{d\lambda}\frac{dx^{\sigma}}{d\lambda} + f^{-1}\left(\delta^{\rho}_{\mu}\nabla_{\nu}f + \delta^{\rho}_{\nu}\nabla_{\mu}f - g_{\mu\nu}g^{\rho\lambda}\nabla_{\lambda}f\right)\frac{dx^{\rho}}{d\lambda}\frac{dx^{\sigma}}{d\lambda} = 0. \tag{1.4.8}$$

In natural units ($c = k = \hbar = 1$),[8] we have the following useful dimensional analysis:

$$[energy] = [mass] = [(frequency)] = [(length)^{-1}] = [(density)^{4}] = [(Time)^{-1}]. \tag{1.4.9}$$

Expressing in mass units, we obtained the dimensional analysis,

$$[S] = [E][T] = M^{0} \tag{1.4.10}$$

and

$$[d^4x] = M^{-4} \to [L] = M^{4} \to [V] = M^{4} \to [\phi] = M^{1}. \tag{1.4.11}$$

The coupling of scalar fields to matter, most often than not, results in violations of the Equivalence principle. The fact that Einstein's theory of gravitation has passed all tests it has ever been subjected to and given that it can account for all behaviours of the gravitational field in the solar system have led to severe constraints being placed on all new theories of gravitation. Any violation of these constraints, particularly the Equivalence principle, is regarded as the discovery of a new force of nature (the so-called fifth force).

A way of quantifying this fifth force is through the Yukawa potential between two test masses m_1, and m_2 with separation r (Adelberger et al., 2003). That is,

$$V(r) = -G_N\frac{m_1m_2}{r}\Big[1 + \alpha e^{-\frac{r}{\lambda}}\Big]. \tag{1.4.12}$$

α is the coupling constant (which measures the strength of the interaction and it is zero for Einstein's theory). λ is the range of interaction and G_N is the usual Newtonian gravitational constant.

Finding the fifth force from the potential is straightforwardly

$$F(r) = -\nabla V(r) = -G(r)\frac{m_1m_2}{r^2}\hat{r}. \tag{1.4.13}$$

Where,

$$G(r) = G_N\Big[1 + \alpha(1 + \frac{r}{\lambda})e^{-\frac{r}{\lambda}}\Big]. \tag{1.4.14}$$

Since Einstein's theory of general relativity is in perfect agreement with all observation data from the laboratory and solar system, modifying it by the addition of scalar fields has to be done in such a way as to leave its behaviours in the laboratory and solar system intact while adjusting its behaviours to agree with cosmic observations. Such modifications of Einstein's field theories are sublimely done by Chameleon field theories.

[8] See P.50 of Sean Carroll's lovely book,"Spacetime and Geometry",(Carroll, 2004), for details

2. Chameleon Field Theories and Profiles

2.1 Chameleon Field Equations

For Chameleon models, the actions we will considered are:[1]

$$\begin{aligned} S &= \int d^4x\sqrt{-g}\Big\{\frac{1}{16\pi G}R - \frac{1}{2}\nabla_\mu\phi\nabla^\mu\phi - V(\phi)\Big\} - \int d^4x \mathcal{L}_m(\psi_m^{(i)}, g_{\mu\nu}^{(i)}) \\ &= \int d^4x\sqrt{-g}\Big\{\frac{M_{pl}^2}{2}R - \frac{1}{2}\nabla_\mu\phi\nabla^\mu\phi - V(\phi) - \frac{1}{\sqrt{-g}}\mathcal{L}_m(\psi_m^{(i)}, g_{\mu\nu}^{(i)})\Big\}. \end{aligned} \tag{2.1.1}$$

$M_{pl} = (8\pi G)^{-\frac{1}{2}}$ is the reduced Planck mass, $\mathcal{L}_m$ is the Lagrangian for the matter fields for each particle species i. $\Psi^{(i)}$ coupled directly to the real scalar field ϕ through the equation

$$g_{\mu\nu}^{(i)} = e^{\frac{2\beta_i\phi}{M_{pl}}} g_{\mu\nu}, \tag{2.1.2}$$

β_i is the dimensionless chameleon coupling for matter species i and it is assumed that $\phi > 0$.

Although $V(\phi)$ can be any potential satisfying the conditions:

$$\beta_i V_{,\phi} < 0, \qquad \frac{V_{,\phi\phi\phi}}{V_{,\phi}} > 0, \qquad \text{and } V_{,\phi\phi} > 0, \tag{2.1.3}$$

the inverse power-law potential (or so-called Ratra-Peebles potential),

$$V(\phi) = M^{4+n}\phi^{-n} \tag{2.1.4}$$

is the potential we are going to use in this essay. M is of mass units, n is a positive constant and we assume that $\beta > 0$ (or $V_{,\phi} < 0$).

As stated in (1.4.3), the equation of motion describing the dynamics of ϕ can be obtained by varying the action with respect to ϕ.

To do this, we are going to Closely follow the procedures used in (Waterhouse, 2006).

Varying the action with respect to ϕ can be done as follows:

$$\begin{aligned} \delta S &= \int d^4x\sqrt{-g}\Bigg\{\delta(-\frac{1}{2}\nabla\phi\nabla^\mu\phi) - V_{,\phi}(\phi)\delta\phi - \frac{1}{\sqrt{-g}}\delta\Big(\mathcal{L}_m(\psi_m^{(i)}, g_{\mu\nu}^{(i)})\Big)\Bigg\} \\ &= \int d^4x\sqrt{-g}\Bigg\{ - \nabla_\mu\phi\delta\nabla^\mu\phi - V_{,\phi}(\phi)\delta\phi - \sum_i \frac{1}{\sqrt{-g}}\frac{\partial\mathcal{L}_m}{\partial g_{\mu\nu}^{(i)}}\frac{\partial g_{\mu\nu}^{(i)}}{\partial\phi}\delta\phi\Bigg\} \\ &= \int d^4x\sqrt{-g}\Bigg\{ - \nabla_\mu\phi\nabla^\mu\delta\phi - V_{,\phi}(\phi)\delta\phi - \sum_i \frac{1}{\sqrt{-g}}\frac{\partial L_m}{\partial g_{\mu\nu}^{(i)}}\frac{2\beta_i}{M_{pl}}g_{\mu\nu}^{(i)}\delta\phi\Bigg\}, \end{aligned} \tag{2.1.5}$$

where $V_{,\phi} \equiv \dfrac{dV}{d\phi}$.

[1] Actions as used in (Khoury and Weltman, 2004b)

The first term on the right hand side side of (2.1.5) can be integrated by parts:

$$\int d^4x\sqrt{-g}(-\nabla_\mu\phi\nabla^\mu\delta\phi) = \int d^4x\sqrt{-g}d(-\nabla_\mu\phi\nabla^\mu\phi) + \int d^4x\sqrt{-g}(\nabla_\mu\nabla^\mu\delta\phi). \tag{2.1.6}$$

Assuming that $\nabla^\mu\phi \to 0$ at infinity or at the boundaries then

$$\int d^4x\sqrt{-g}(-\nabla_\mu\phi\nabla^\mu\delta\phi) = \int d^4x\sqrt{-g}(\nabla_\mu\nabla^\mu\delta\phi). \tag{2.1.7}$$

Substituting (2.1.7) into (2.1.5) yields:

$$\begin{aligned}\delta S &= \int d^4x\sqrt{-g}\left\{(\nabla_\mu\nabla^\mu\phi)\delta\phi - V_{,\phi}(\phi)\delta\phi - \sum_i \frac{1}{\sqrt{-g}}\frac{\partial\mathcal{L}_m}{\partial g^{(i)}_{\mu\nu}}\frac{2\beta_i}{M_{pl}}g^{(i)}_{\mu\nu}\delta\phi\right\}\\ &= \int d^4x\sqrt{-g}\left\{\nabla_\mu\nabla^\mu\phi - V_{,\phi}(\phi) - \sum_i \frac{1}{\sqrt{-g}}\frac{\partial\mathcal{L}_m}{\partial g^{(i)}_{\mu\nu}}\frac{2\beta_i}{M_{pl}}g^{(i)}_{\mu\nu}\right\}\delta\phi\end{aligned} \tag{2.1.8}$$

Given that nearly all tests of gravity are carried out in regions of negligible small density (vacuum or Space) or since solar system can be approximated to be within the weak gravitational field limit, we can to good approximation assume that the fields are static[2] (1.2.9). With this approximation, (2.1.8) can be written as

$$\frac{1}{\sqrt{-g}}\frac{\delta S}{\delta\phi} = \nabla^2\phi - V_{,\phi}(\phi) - \sum_i \frac{1}{\sqrt{-g}}\frac{\partial\mathcal{L}_m}{\partial g^{(i)}_{\mu\nu}}\frac{2\beta_i}{M_{pl}}g^{(i)}_{\mu\nu} = 0. \tag{2.1.9}$$

That is,

$$\nabla^2\phi - V_{,\phi}(\phi) - \sum_i \frac{1}{\sqrt{-g}}\frac{\partial\mathcal{L}_m}{\partial g^{(i)}_{\mu\nu}}\frac{2\beta_i}{M_{pl}}g^{(i)}_{\mu\nu} = 0 \tag{2.1.10}$$

or

$$\nabla^2\phi = V_{,\phi}(\phi) + \sum_i \frac{1}{\sqrt{-g}}\frac{\partial\mathcal{L}_m}{\partial g^{(i)}_{\mu\nu}}\frac{2\beta_i}{M_{pl}}g^{(i)}_{\mu\nu}. \tag{2.1.11}$$

If $\tilde{g}$ denotes the determinant of the metric $g^{(i)}_{\mu\nu}$, then it is straightforward to show that

$$\tilde{g} = e^{\frac{8\beta_i\phi}{M_{pl}}}g. \tag{2.1.12}$$

From (1.4.4) and (2.1.12), we see that

$$\frac{2}{\sqrt{-g}}\frac{\partial\mathcal{L}_m}{\partial g^{(i)}_{\mu\nu}} = e^{\frac{4\beta_i\phi}{M_{pl}}}\frac{2}{\sqrt{-\tilde{g}}}\frac{\partial\mathcal{L}_m}{\partial g^{(i)}_{\mu\nu}} = -e^{\frac{4\beta_i\phi}{M_{pl}}}T^{\mu\nu}_{(i)}. \tag{2.1.13}$$

With this, (2.1.11) can be rewritten as

$$\nabla^2\phi = V_{,\phi}(\phi) - \sum_i \frac{\beta_i}{M}e^{\frac{4\beta_i\phi}{M_{pl}}}g^{(i)}_{\mu\nu}T^{\mu\nu}_{(i)}. \tag{2.1.14}$$

For non-relativistic matter,

$$g^{(i)}_{\mu\nu}T^{\mu\nu}_{(i)} \approx -\tilde{\rho}_i, \tag{2.1.15}$$

[2] In realistic cases, the cosmological geometry is time dependent

where $\tilde{\rho}_i$ is the energy density of the i^{th} particle in the Jordan frame.

To isolate and identify the matter contents from ϕ, in order to lay bare the chameleon behaviour of the $\phi-$ fields, it is instructive and convenient to write $\tilde{\rho}_i$ in term of ρ_i, the conserved energy density in the Einstein frame. That is,

$$\rho_i \equiv \tilde{\rho}_i e^{\frac{3\beta_i \phi}{M_{pl}}}. \tag{2.1.16}$$

Putting (2.1.16) into (2.1.14) gives

$$\nabla^2 \phi = V_{,\phi}(\phi) + \sum_i \rho_i \frac{\beta_i}{M_{pl}} e^{\frac{\beta_i \phi}{M_{pl}}}. \tag{2.1.17}$$

(2.1.17) could also be expressed in terms of an effective potential

$$V_{eff}(\phi) = V(\phi) + \sum \rho_i e^{\frac{\beta_i \phi}{M_{pl}}}. \tag{2.1.18}$$

The effective potential is density dependent! This astonishing result, which happens to be the source of the name Chameleon, is one of the distinct features of the chameleon.

(2.1.17) could now be written as:

$$\nabla^2 \phi = V_{eff}(\phi). \tag{2.1.19}$$

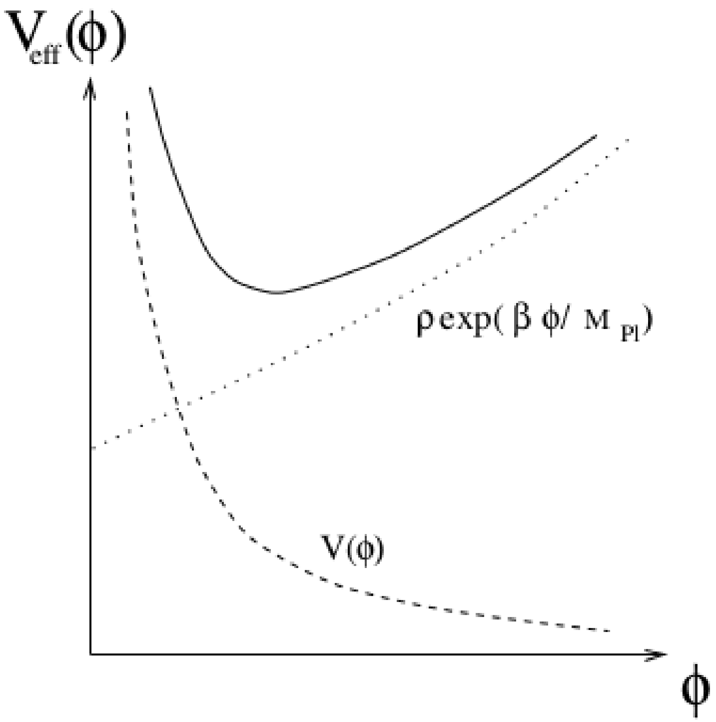

Figure 2.1: The effective potential(broad curve) as a function of the bare potential(dashed curve) and the ambient density (dotted curve). (Khoury and Weltman, 2004b)

The plot of $V_{eff}(\phi)$, as shown in Figure 2.1, illustrates that even though the bare potential($V(\phi)$) is monotonic, the effective potential($V_{eff}(\phi)$) exhibits a minimum which we will denoted as ϕ_{min}.

In other words,

$$V_{eff,\phi}(\phi_{min}) \equiv 0 \tag{2.1.20}$$

or

$$V_{,\phi}(\phi_{min}) + \sum_i \rho_i \frac{\beta_i}{M_{pl}} e^{\frac{\beta_i \phi_{min}}{M_{pl}}} = 0. \tag{2.1.21}$$

The mass of small fluctuations about ϕ_{min} is defined as

$$m^2_{min} \equiv V_{eff,\phi}(\phi_{min}) = V_{,\phi\phi}(\phi_{min}) + \sum_i \rho_i \frac{\beta_i^2}{M_{pl}^2} e^{\frac{\beta_i \phi_{min}}{M_{pl}}}. \tag{2.1.22}$$

If we assume that

$$|\beta_i \phi_{min}| \ll M_{pl} \qquad \text{and} \qquad |V_{,}\phi\phi| \gg \left|\rho \frac{\beta_i^2}{M_{pl}^2}\right|, \tag{2.1.23}$$

then

$$m^2_{min} \sim V_{,\phi}(\phi_{min}). \tag{2.1.24}$$

Also, very close to the minimum,

$$\phi \sim \phi_{min}. \tag{2.1.25}$$

As shown by the two equations,(2.1.21), (2.1.22) and vividly illustrated by Figure 2.2 and by the runaway nature of the bare potential, larger ρ_i means larger m_{min} but smaller ϕ and vice versa.

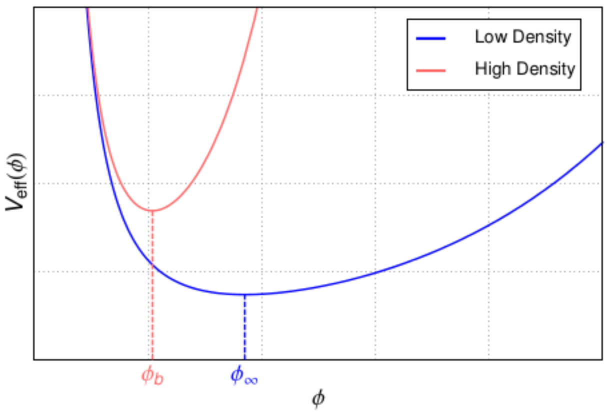

Figure 2.2: Illustration of the relationship among ϕ_{min}(where ϕ_b is ϕ_{min} inside a compact object and ϕ_∞ at ϕ_{min} outside the compact object) and ρ. (Hees and Füzfa, 2012)

2.2 Field Profiles for Compact Objects

As was done in (Khoury and Weltman, 2004b), we restrict our analysis to the static case and consider a spherically symmetric body [3] of radius R_b, homogeneous density $\rho_b$and total mass $M_b = \frac{4\pi\rho_b R_c^3}{3}$, which is embedded in a surrounding of homogeneous density ρ_∞.

By assuming that the compact body is not affected by the presence of other compact bodies, we can write (2.1.17) as:

$$\frac{d^2\phi}{dr^2} + \frac{2}{r}\frac{d\phi}{dr} = V_{,\phi} + \frac{\beta}{M_{pl}}\rho(r)e^{\frac{\beta\phi}{M_{pl}}} \tag{2.2.1}$$

Where:

$$\rho(r)\Big|_{r<R_b} \equiv \rho_b \tag{2.2.2}$$

$$\rho(r)\Big|_{r>R_b} \equiv \rho_\infty \tag{2.2.3}$$

$$V_{eff}(\phi_{min})\Big|_{r<R_b} \equiv \phi_b \tag{2.2.4}$$

$$V_{eff}(\phi_{min})\Big|_{r>R_b} \equiv \phi_\infty \tag{2.2.5}$$

$$V_{eff,\phi\phi}(\phi_{min})\Big|_{r<R_b} \equiv m_b \tag{2.2.6}$$

$$V_{eff}(\phi_{min})\Big|_{r>R_b} \equiv m_\infty. \tag{2.2.7}$$

The the boundary conditions for (2.2.1) are:

$$\frac{d\phi}{dr}\Big|_{r=0} = 0 \tag{2.2.8}$$

and

$$\lim_{r\to\infty}\phi(r) = \phi_\infty. \tag{2.2.9}$$

The $\phi-$ profile for a compact body depends on the magnitude of the product $R_b M_b$. The values for $R_b M_b$ (whose meaning will soon be made clearer) determines whether a compact body has thin-shell or thick-shell.

Unlike an object with thick-shell, which has the same profile throughout its interior, the $\phi-$ profile for an object that suffers from a thin-shell effect depends on how close to the minimum of the effective potential, V_{eff}, the ϕ-field is.

In light of this, the interior of a compact object with thin-shell can be divided into two intervals, say $[0, R_s]$ and $[R_s, R_b]$. R_s is defined such that $0 < r < R_s$ constitutes what is meant by close to minimum of the potential.

For $0 < r < R_s$, the field is approximately constant and is

$$\phi \sim \phi_b \qquad \text{for } 0 < r < R_s. \tag{2.2.10}$$

[3] to excellent approximation,the Sun and all planetary bodies in the solar can be considered to be spherical symmetric and the field outside of them can be considered static (Birkhoff's theorem).

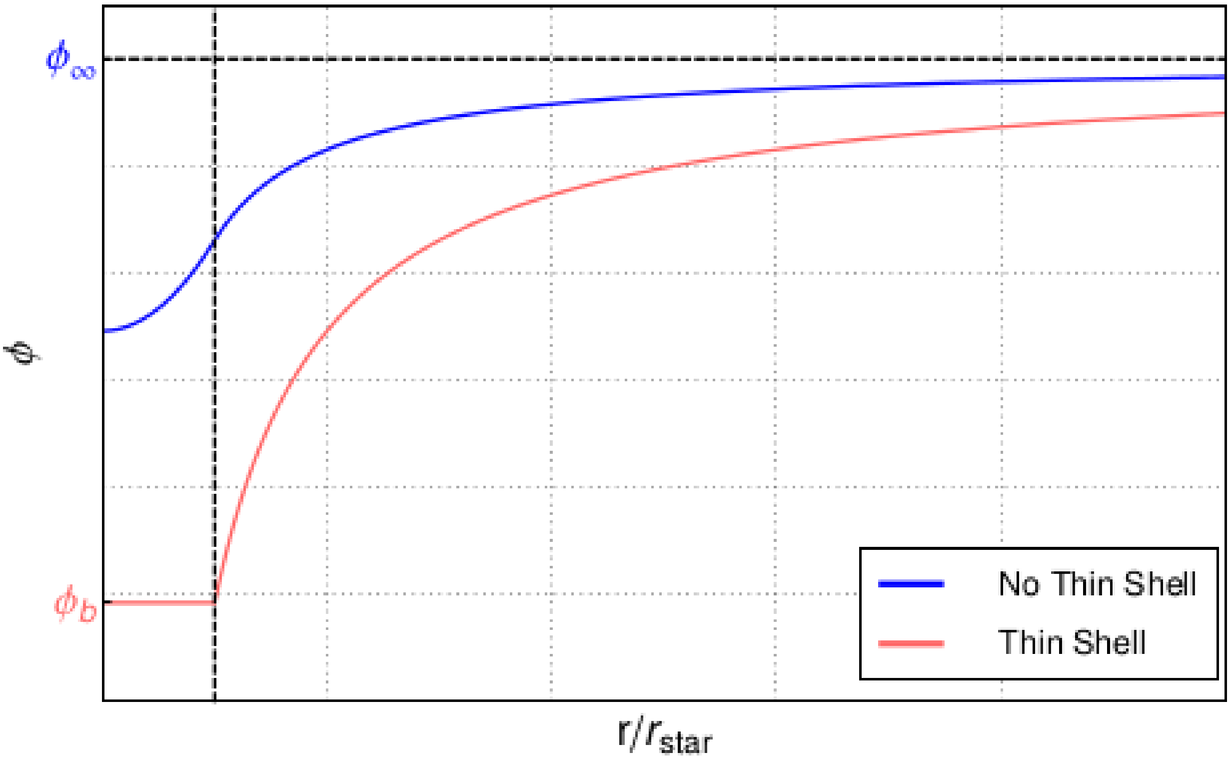

Figure 2.3: The ϕ-field is frozen at minimum of the effective potential for the the thin-shell but it does not reach the minimum for the thick-shell (Hees and Füzfa, 2012)

Far away from the minimum of the effective potential (or in the interval $[R_s, R_b]$), as can be seen in Figure 2.1, the bare potential, $V(\phi)$, decays rapidly. This means, for $\phi \gg \phi_b$

$$\frac{\beta}{M_{pl}}\rho e^{\frac{\beta\phi}{M_{pl}}} \gg \Big|V_{,\phi}(\phi)\Big| \tag{2.2.11}$$

and in such a case, $\Big|V_{,\phi}(\phi)\Big|$ can be neglected. Also, assuming that $\phi \ll M_{pl}$, (which is often the case for Chameleon models) (2.2.1) becomes:

$$\frac{d^2\phi}{dr^2} + \frac{2}{r}\frac{d\phi}{dr} = \frac{\beta}{M_{pl}}\rho_b. \tag{2.2.12}$$

(2.2.12) can be solved as follows:

$$\frac{d^2\phi}{dr^2} + \frac{2}{r}\frac{d\phi}{dr} = \frac{1}{r^2}d\Big(r^2\frac{d\phi}{dr}\Big) = \frac{\beta}{M_{pl}}\rho_b.$$

$$d\Big(r^2\frac{d\phi}{dr}\Big) = \frac{\beta r^2}{M_{pl}}\rho_b$$

$$r^2\frac{d\phi}{dr} = \frac{\beta}{3M_{pl}}\rho_b r^3 + A. \tag{2.2.13}$$

A is an integration constant.

Subjecting (2.2.13) to the boundary condition (2.2.8), we get

$$A = -\frac{\beta\rho_b}{3M_{pl}}R_s^3. \tag{2.2.14}$$

With (2.2.14), (2.2.13) becomes

$$r^2\frac{d\phi}{dr} = \frac{\beta}{3M_{pl}}\rho_b(r^3 - R_s^3),$$

which is the same as

$$\frac{d\phi}{dr} = \frac{\beta}{3M_{pl}}\rho_b\left(r - \frac{R_s^3}{r^2}\right). \tag{2.2.15}$$

Integrating (2.2.15) yields:

$$\phi(r) = \frac{\beta}{3M_{pl}}\rho_b\left(\frac{r^2}{2} + \frac{R_s^3}{r}\right) + B, \tag{2.2.16}$$

where B is an integration constant.

Using the boundary condition $\phi(r = R_s) = \phi_b$, gives

$$B = \phi_b - \frac{\beta\rho_b}{2M_{pl}}R_s^3. \tag{2.2.17}$$

Substituting (2.2.17) into (2.2.16) gives

$$\phi(r) = \frac{\beta}{3M_{pl}}\rho_b(\frac{r^2}{2} + \frac{R_s^3}{r}) - \frac{\beta\rho_b R_s^2}{2M_{pl}} + \phi_b \approx \phi_b \qquad \text{for } R_s < r < R_b. \tag{2.2.18}$$

Equations (2.2.10) and (2.2.18) are the field profiles for the interior ($r < R_b$) of a compact object with thin-shell.

From (2.2.9), it is clear that far away from a compact object ($r \gg R_b$) the field profile is

$$\phi \sim \phi_\infty \tag{2.2.19}$$

but very close to the minimum of the potential (outside the compact object) the effective potential can be approximated as a harmonic potential. That is,

$$V_{eff,\phi} = m_\infty^2(\phi - \phi_\infty). \tag{2.2.20}$$

Substituting (2.2.20) into (2.1.19) gives

$$\frac{d^2\phi}{dr^2} + \frac{2}{r}\frac{d\phi}{dr} = m_\infty^2(\phi - \phi_\infty). \tag{2.2.21}$$

Making the ansatz

$$\phi(r) = \frac{e^{k(r-R_b)}}{r} + \phi_\infty, \tag{2.2.22}$$

where k is a constant to be determined, then

$$\frac{d\phi}{dr} = \frac{kre^{k(r-R_b)} + e^{k(r-R_b)}}{r^2} = \frac{kr-1}{r^2}e^{k(r-R_b)}, \tag{2.2.23}$$

$$d\Big(\frac{kr-1}{r^2}\Big) = \frac{r^2k - 2r(kr-1)}{r^4} = \frac{2-kr}{r^3} \tag{2.2.24}$$

and

$$\frac{d^2\phi}{dr^2} = \frac{kr^2-k}{r^2}e^{k(r-R_b)} + e^{k(r-R_b)}d\Big(\frac{kr-1}{r^2}\Big). \tag{2.2.25}$$

(2.2.24) into (2.2.25) gives

$$\begin{aligned}\frac{d^2\phi}{dr^2} &= \frac{kr^2-k}{r^2}e^{k(r-R_b)} + \frac{2-kr}{r^3}e^{k(r-R_b)} \\ &= \frac{k^2r^2-2kr+2}{r^3}e^{k(r-R_b)}.\end{aligned} \tag{2.2.26}$$

Putting (2.2.22), (2.2.23) and (2.2.26) into(2.2.21) gives

$$\frac{k^2r^2-2kr+2}{r^3}e^{k(r-R_b)} + \frac{kr-1}{r^2}e^{k(r-R_c)} = m_\infty^2\frac{e^{k(r-R_b)}}{r}$$

$$\frac{k^2r^2-2kr+2+2kr-2}{r^3}e^{k(r-R_b)} = m_\infty^2\frac{e^{k(r-R_b)}}{r} \Rightarrow k^2 = m_\infty^2$$

or

$$k = \pm m_\infty. \tag{2.2.27}$$

Thus, with (2.2.27), (2.2.22) becomes:

$$\phi(r) = \frac{Ae^{-m_\infty(r-R_b)}}{r} + \frac{Be^{m_\infty(r-R_b)}}{r} + \phi_\infty. \tag{2.2.28}$$

Taking the boundary conditions

$$\lim_{r\to\infty}\phi(r) = \phi_\infty,$$

leads to $B = 0$.

Thus, the field profile for the region outside a compact object suffering from thin-shell effect is

$$\phi(r) = \frac{Ae^{-m_\infty(r-R_b)}}{r} + \phi_\infty \qquad \text{for } r > R_b. \tag{2.2.29}$$

The profiles for the interior and the profiles for the exterior of a compact object with thin-shell can be matched at $r = R_b$ as follows:

$$\phi(r=R_b) = \frac{\beta\rho_b}{6M_{pl}}(R_s^2+2R_s^2) - \frac{\beta\rho_b}{2M}R_s^2 + \phi_b = \phi_b = \frac{A}{R_b} + \phi_\infty \tag{2.2.30}$$

or

$$A = -R_b(\phi_\infty - \phi_b). \tag{2.2.31}$$

Substituting for A in (2.2.29) gives

$$\phi(r) = \frac{-R_b(\phi_\infty - \phi_b)e^{-m_\infty(r-R_b)}}{r} + \phi_\infty. \tag{2.2.32}$$

With hindsight, we can define the contrast between the field outside and inside minimum for the compact object by:

$$\phi_\infty - \phi_b \equiv 6\beta M_{pl}\Phi_b \frac{\Delta R_b}{R_b}. \tag{2.2.33}$$

Where ΔR_b has been defined as:

$$\Delta R_b = R_b - R_s. \tag{2.2.34}$$

The magnitude of the ratio of this difference in minimum field values to the radius R_b of the compact object determines whether the compact has thin-shell or thick-shell. That is, any compact object with

$$\frac{\Delta R_b}{R_b} \equiv \frac{\phi_\infty - \phi_b}{6\beta M_{pl}\Phi_b} \ll 1 \tag{2.2.35}$$

manifests a thin-shell effect.

The thin-shell is the other unique feature of the chameleon.

$$\Phi_b = \frac{GM_c}{R_b} = \frac{M_b}{8\pi M_{pl}^2 R_b} \tag{2.2.36}$$

is the Newtonian potential of the Compact object.

so,

$$R_b(\phi_\infty - \phi_b) = 6\frac{R_b^3\beta M_{pl}\Phi_b}{R_b^2}\frac{\Delta R_b}{R_b} = \frac{R_b^3 6\beta M_{pl} M_b}{8\pi M_{pl}^2 R_b^3}\frac{\Delta R_b}{R_b} = \Big(\frac{\beta}{4\pi M_{pl}}\Big)\Big(\frac{3\Delta R_b}{R_b}\Big)M_b. \tag{2.2.37}$$

(2.2.37) into (2.2.32) gives:

$$\phi(r) \approx -\Big(\frac{\beta}{4\pi M_{pl}}\Big)\Big(\frac{3\Delta R_b}{R_b}\Big)M_b\frac{e^{-m_\infty(r-R_b)}}{r} + \phi_\infty \qquad \text{for } r > R_b. \tag{2.2.38}$$

As we shall soon see, (2.2.38) is one of the most important equations, if not the most important, in applications of the Chameleon model to the solar system. For it describes the profiles generated by all bodies with thin-shell, including Sun, Moon and planets.

If $R_s = 0$ then the division of the radius of compact object into intervals becomes superfluous and a single profile suffices for the entire interval $0 < r < R_b$.

This single profile for the thick-shell compact object is obtained by simply replacing R_s by 0 and replacing ϕ_b by ϕ_i where

$$\phi(r = 0) \equiv \phi_i \tag{2.2.39}$$

in (2.2.18) to obtain:

$$\phi(r) = \frac{\beta\rho_b r^2}{6M_{pl}} + \phi_i \qquad \text{for } 0 < r < R_b. \tag{2.2.40}$$

Also, the profile for the exterior of a compact object with thick-shell can also be found simply by replacing R_s by 0 in (2.2.38) or $3\Delta R_c \approx R_b$. Thus, giving:

$$\phi(r) \approx -\left(\frac{\beta}{4\pi M_{pl}}\right)\frac{M_b e^{-m_\infty(r-R_b)}}{r} + \phi_\infty \qquad \text{for } r > R_b. \tag{2.2.41}$$

(2.2.41) is also very important. While (2.2.38) is used to verify that the Chameleon model is in perfect agreement with Einstein's theory of General Relativity and Newtonian Mechanics in arenas were Einstein's and Newton's theories are valid,(2.2.41) is purported to be valid in arenas were even Einstein's great theory is found wanting.

To have concrete idea on the meaning of the profile of a compact object and see the thin-shell effect at work, let's recap the analysis of the profiles for ϕ inside and in the vicinity of the Earth as done in (Khoury and Weltman, 2004b).

The Earth can be modelled as a solid sphere of radius $R_\oplus = 6 \times 10^8 cm$ and homogeneous density $\rho_\oplus = 10g/cm^3$. The atmosphere of the Earth can be approximated to have a radius, $R_{moon} = 10km$ thick and a homogeneous density $\rho_{atm} = 10^{-3}g/cm^3$.

Though Earth is assumed to not be affected by neighbouring compact objects, it is embedded in a homogeneous density of dark energy whose density is $\rho_G = 10^{-24}g/cm^3$. $\phi_\oplus$, ϕ_{atm}, and ϕ_G are the field values which minimize the effective potential for the neighbourhood, Earth and atmosphere respective and $m_\oplus$, m_{atm} and m_G are their associated masses.

Since the atmosphere has a thin-shell[4], in the most of the atmosphere

$$\phi \approx \phi_{atm}.$$

Also, since the Earth is denser than its atmosphere, it follows from (2.2.35) and (2.2.36) that the Earth has a thin-shell. In which case, we are justified in writing

$$\phi \approx \phi_\oplus \qquad \text{for } r < R_\oplus. \tag{2.2.42}$$

In order for the atmosphere to have a thin shell, the thickness of the shell must be less than the thickness of the atmosphere itself. That is,

$$\Delta R_{atm} \approx 10^{-3} R_{atm}.$$

Hence,

$$\frac{\Delta R_{atm}}{R_{atm}} \leq 10^{-3} \tag{2.2.43}$$

From (2.2.35), the thin-shell condition for the atmosphere reads

$$\frac{\Delta R_{atm}}{R_{atm}} = \frac{\phi_G - \phi_{atm}}{6\beta M_{pl}\Phi_{atm}} \ll 1. \tag{2.2.44}$$

Where,

$$\Phi_{atm} = \frac{GM_{atm}}{R_{atm}} = \frac{M_{atm}}{8\pi M_{pl}^2 R_{atm}} = \frac{\rho_{atm}\frac{4\pi R_{atm}^3}{3}}{8\pi M_{pl}^2 R_{atm}} = \frac{\rho_{atm} R_{atm}^2}{6M_{pl}^2}. \tag{2.2.45}$$

[4]see (Khoury and Weltman, 2004b) for proof and detailed

Using the data, $\rho_{atm} \approx 10^{-4}\rho_{\oplus}$ and $\frac{\Phi_{atm}}{\Phi_{\oplus}} = \left(\frac{\rho_{atm} R_{atm}^2}{6M_{pl}^2}\right)\left(\frac{6M_{pl}^2}{\rho_{\oplus} R_{\oplus}^2}\right) \approx \frac{\rho_{atm}}{\rho_{\oplus}} \approx 10^{-4}$ or $\Phi_{atm} \approx 10^{-4}\Phi_{\oplus}$, we can now write

$$\frac{\Delta R_{\oplus}}{R_{\oplus}} = \frac{\phi_G - \phi_{atm}}{6\beta M_{pl}\Phi_{\oplus}} \leq 10^{-7}. \tag{2.2.46}$$

The exterior solution, $r > R_b$ is given by (2.2.38) with $m_\infty = m_G$ and $\phi_\infty = \phi_G$. That is,

$$\phi(r) \approx -\left(\frac{\beta}{4\pi M_{pl}}\right)\left(\frac{3\Delta R_{\oplus}}{R_{\oplus}}\right) M_{\oplus} \frac{e^{-m_G(r-R_{atm})}}{r} + \phi_G \qquad \text{for } r > R_{atm}. \tag{2.2.47}$$

2.3 Field Profiles for the Vacuum Chamber

The Vacuum chamber is modelled in (Khoury and Weltman, 2004b) as a spherical cavity with radius R_{vac} and density $\rho_{vac} = 0$. Also, effects from its walls are ignored. It has been argued[5] that since the effective potential of the field in a perfectly empty vacuum has no extrema, the curvature of the potential in it has to be of the order R_{vac}^{-2}. Also, according to (Khoury and Weltman, 2004b), numerical analysis of of the equation for ϕ within the vacuum chamber, (2.2.12), confirms that:

1. the chameleon assumes the value $\phi \sim \phi_{vac}$ within the vacuum chamber where ϕ_{vac} satisfies

$$m^{-1}(\phi_{vac}) \equiv V_{,\phi\phi}^{-\frac{1}{2}} = R_{vac}$$

2. throughout the Chamber, ϕ varies slowly, with $\left|\frac{d\phi}{dr}\right| \leq \frac{\phi_{vac}}{R_{vac}}$ and

3.outside the chamber the solution tends to ϕ_{atm} within a distance of m_{atm}^{-1} from the walls.

Actually, the only real difference between our modelled vacuum chamber and compact object, save the vacuum being assumed perfectly empty, is that $\rho_{vac} \ll \rho_\infty$ whereas $\rho_\infty \ll \rho_b$ for the compact object. So, it is logical to conclude that both have similar profiles for their less denser regions and similar profile for their denser regions. That is, the profile for the exterior of the compact object is similarly to the profile for the interior of the vacuum.

In other words, the profile that a test body of mass M_c,radius R_c with thin-shell generates when place in our modelled vacuum chamber is

$$\phi \approx -\left(\frac{\beta}{4\pi M_{pl}}\right)\left(\frac{3\triangle R_b}{R_c}\right)\frac{M_b e^{-\frac{r}{R_{vac}}}}{r} + \phi_{vac}. \tag{2.3.1}$$

While, those generated by a test body of mass M_c,radius R_c with thick-shell is

$$\phi \approx -\left(\frac{\beta}{4\pi}\right)\left(\frac{M_c}{M_{pl}}\right)\frac{e^{-\frac{r}{R_{vac}}}}{r} + \phi_{vac}. \tag{2.3.2}$$

[5] from an intuitive point of view, the argument is that the only length scale associated with the vacuum chamber is its radius, R_{vac}. See (Khoury and Weltman, 2004b) for details.

We have ignored the profiles for $r \gg R_{vac}$, which contributes negligibly to the profiles for the vacuum chamber.

Given the sensitivity of tests of the equivalence principle, these tests have to be greatly isolated from external influence (particularly in the laboratory) thus making the vacuum chamber the ideal place for such tests.

These profiles and their thin-shell/thick-shell effect have been confirmed to be correct by numerical stimulations and by plots of these profiles with real and reasonable data (Khoury and Weltman, 2004b), (Brax et al., 2010)(Babichev and Langlois, 2010)(Tsujikawa et al., 2009) (Hees and Füzfa, 2012).

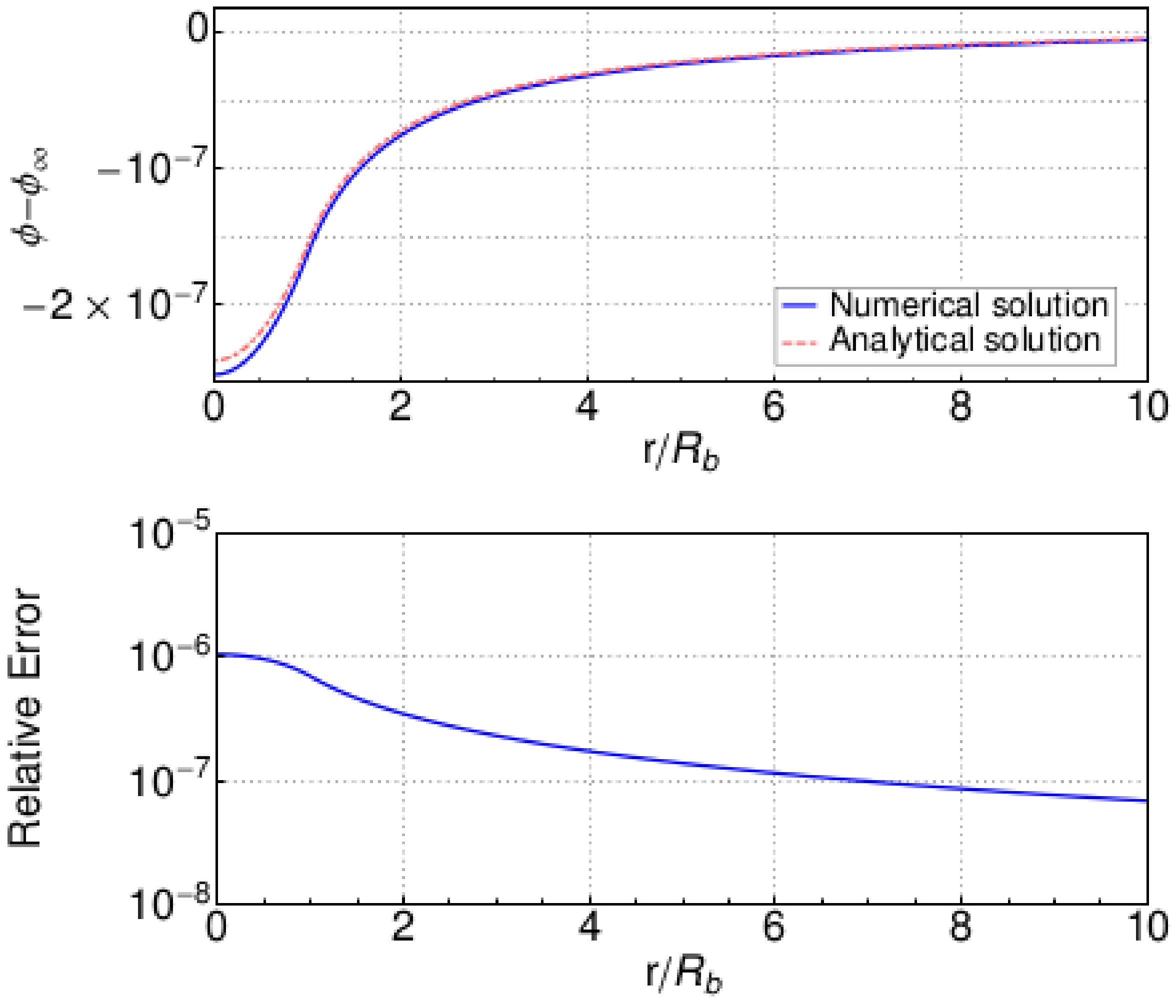

Figure 2.4: Top:Comparison the numerical stimulation and analytical approximation of the field profile around the sun, when the sun is assumed to have a thick-shell. Bottom: relative difference between the numerical solution and analytical approximation. (Hees and Füzfa, 2012).

These detailed calculations and analyses show unambiguously that the thin-shell mechanism is real and that the profiles we have derived crudely provide very good approximations to the ϕ field generated by compact objects and vacuum chambers and thus we can go out enough confidence and test the Chameleon model we have been discussing .

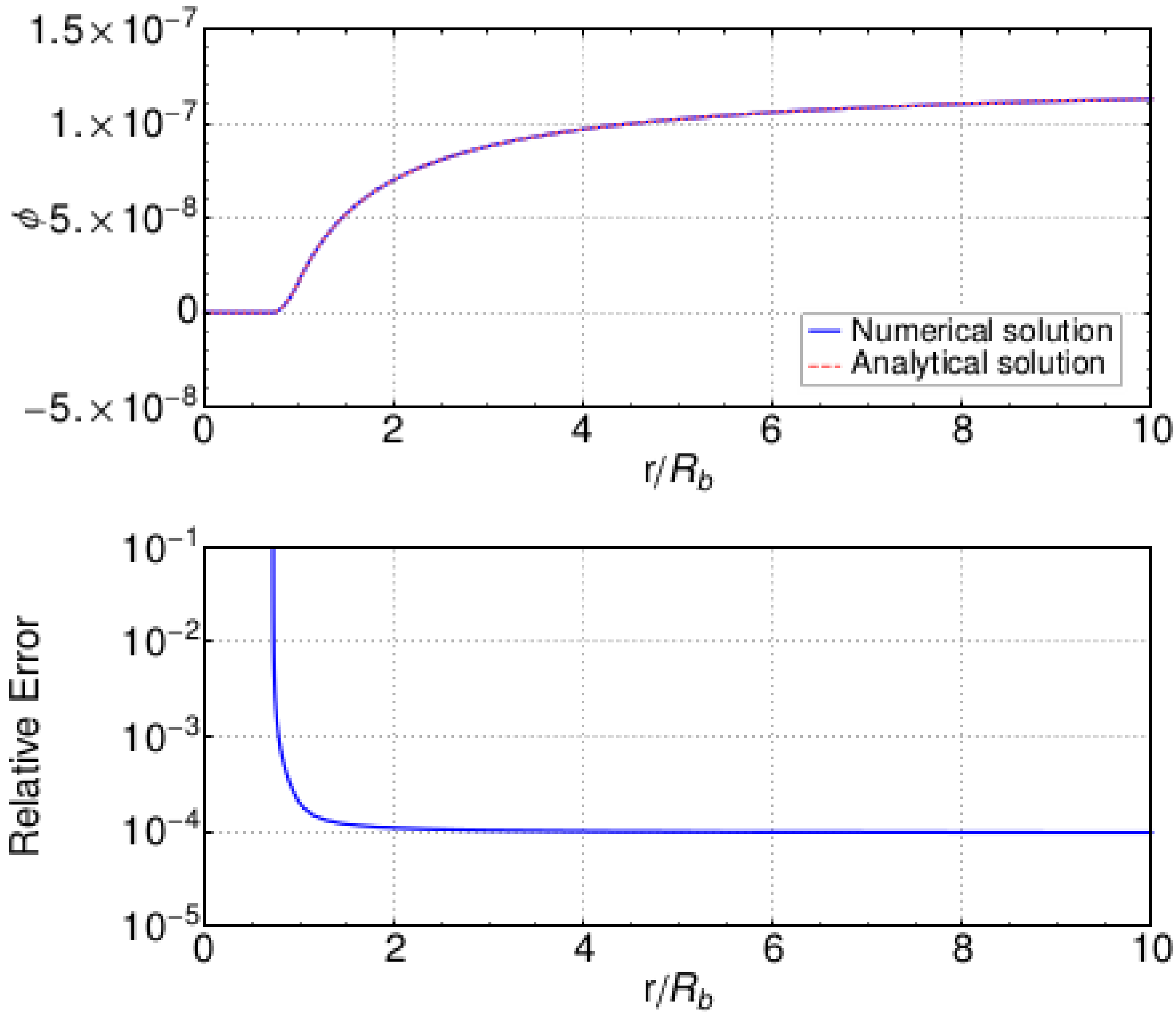

Figure 2.5: Top:Comparison the numerical stimulation and analytical approximation of the field profile, when the sun is assumed to have a thin-shell. Bottom: relative difference between the numerical solution and analytical approximation (Hees and Füzfa, 2012).

3. Fifth Force and Tests

3.1 The Chameleon Force

It was previously discussed that (1.4.7) is the geodesic equation in the Jordan frame for the worldline x^μ of a test particle.

Comparing (1.4.2) and(2.1.2) shows that,

$$f = e^{\frac{\beta_i \phi}{M_{pl}}}. \tag{3.1.1}$$

So, $f^{-1} = e^{-\frac{\beta_i \phi}{M_{pl}}}$, $\nabla_\nu f = f_{,\phi}\phi_{,\nu} = \frac{\beta_i}{M_{pl}} e^{\frac{\beta_i \phi}{M_{pl}}} \phi_{,\nu}$, $\nabla_\mu f = f_{,\phi}\phi_{,\mu} = \frac{\beta_i}{M_{pl}} e^{\frac{\beta_i \phi}{M_{pl}}} \phi_{,\mu}$, and $\nabla_\lambda f = f_{,\phi}\phi_{,\lambda} = \frac{\beta_i}{M_{pl}} e^{\frac{\beta_i \phi}{M_{pl}}} \phi_{,\lambda}$.

Substituting these results into (1.4.5) gives

$$\tilde{\Gamma}^\rho_{\mu\nu} = \Gamma^\rho_{\mu\nu} + \frac{\beta_i}{M_{pl}} \Big(\delta^\rho_\mu \phi_{,\nu} + \delta^\rho_\nu \phi_{,\mu} - g_{\mu\nu} g^{\rho\lambda} \phi_{,\lambda} \Big). \tag{3.1.2}$$

With this, (1.4.8) can be written as:

$$\ddot{x}^\rho + \Gamma^\rho_{\mu\nu} \dot{x}^\mu \dot{x}^\nu + \frac{\beta_i}{M_{pl}} \Big(\delta^\rho_\mu \phi_{,\nu} + \delta^\rho_\nu \phi_{,\mu} - g_{\mu\nu} g^{\rho\lambda} \phi_{,\lambda} \Big) \dot{x}^\mu \dot{x}^\nu = 0$$

$$\ddot{x}^\rho + \Gamma^\rho_{\mu\nu} \dot{x}^\mu \dot{x}^\nu + \frac{\beta_i}{M_{pl}} \Big(\phi_{,\nu} \dot{x}^\rho \dot{x}^\nu + \phi_{,\mu} \dot{x}^\mu \dot{x}^\rho - g_{\mu\nu} \dot{x}^\mu \dot{x}^\nu g^{\rho\lambda} \phi_{,\lambda} \Big) = 0$$

$$\ddot{x}^\rho + \Gamma^\rho_{\mu\nu} \dot{x}^\mu \dot{x}^\nu + \frac{\beta_i}{M_{pl}} \Big(\phi_{,\nu} \dot{x}^\rho \dot{x}^\nu + \phi_{,\mu} \dot{x}^\mu \dot{x}^\rho + g^{\rho\lambda} \phi_{,\lambda} \Big) = 0 \tag{3.1.3}$$

Where, we have used (1.2.10).

(3.1.3) can now be written as:

$$\ddot{x}^\rho + \Gamma^\rho_{\mu\nu} \dot{x}^\mu \dot{x}^\nu + \frac{\beta_i}{M_{pl}} \Big(2\phi_{,\mu} \dot{x}^\mu \dot{x}^\rho + g^{\rho\lambda} \phi_{,\lambda} \Big) = 0 \tag{3.1.4}$$

The implication of the above equation is that the coupling of a scalar to the matter field has introduced a fifth force:

$$\frac{\overrightarrow{F}_\phi}{m} = -\frac{\beta_i}{M_{pl}} \nabla \phi. \tag{3.1.5}$$

m is the mass of the test particle and ϕ is the potential for the Chameleon force.

Let's illustrate this for the Earth.

The Earth and its atmosphere have thin-shell, so

$$\phi(r) \approx -\Big(\frac{\beta}{4\pi M_{pl}}\Big)\Big(\frac{3\Delta R_\oplus}{R_\oplus}\Big) M_\oplus \frac{e^{-m_G(r - R_{atm})}}{r} + \phi_G$$

$$\approx -\Big(\frac{\beta}{4\pi M_{pl}}\Big)\Big(\frac{3\Delta R_{\oplus}}{R_{\oplus}}\Big)\frac{M_{\oplus}}{r} + \phi_G \qquad \text{for } r \gg R_{atm} \tag{3.1.6}$$

is the ϕ profile associated with them.

It is straightforward to find the fifth force associated with this profile. Let's run through it.

$$\nabla\phi = \Big(\frac{\beta}{4\pi M_{pl}}\Big)\Big(\frac{3\triangle R_{\oplus}}{R_{\oplus}}\Big)\frac{M_{\oplus}}{r^2}. \tag{3.1.7}$$

(3.1.7) into (3.1.5) gives:

$$F_\phi = -\frac{\beta_i}{M_{pl}}\Big(\frac{\beta}{4\pi M_{pl}}\Big)\Big(\frac{3\triangle R_{\oplus}}{R_{\oplus}}\Big)\frac{M_{\oplus}}{r^2} = 2\beta\beta_i\Big(\frac{3\triangle R_{\oplus}}{R_{\oplus}}\Big)\frac{M_{\oplus}m}{8\pi M_{Pl}^2 r^2} = 2\beta\beta_i\Big(\frac{3\triangle R_{\oplus}}{R_{\oplus}}\Big)F_N \tag{3.1.8}$$

Where

$$F_N \equiv \frac{M_{\oplus}m}{8\pi M_{Pl}^2 r^2} \rightarrow a_N = \frac{M_{\oplus}}{8\pi M_{Pl}^2 r^2} \tag{3.1.9}$$

So, scalar-tensor theories like the Chameleon field theories are expected to have a total force of magnitude:

$$F = \frac{GM_1M_2}{r^2}(1+2\beta_1\beta_2) = \frac{G_{eff}M_1M_2}{r^2} \tag{3.1.10}$$

Where

$$G_{eff} = G(1+2\beta_1\beta_1) \tag{3.1.11}$$

3.2 Laboratory Tests

From (1.4.12), it is clear that modification of Einstein's field equations by the addition of scalar fields lead to the introduction of a fifth force and as previously discussed this fifth force can be parametrized by a Yukawa potential:

$$V(r) = -G_N\frac{m_1m_2}{r}\alpha e^{-\frac{r}{\lambda}} = -\alpha\frac{m_1m_2}{8\pi M_{pl}^2}e^{-\frac{r}{\lambda}} \tag{3.2.1}$$

For $10cm \lesssim \lambda \approx R_{vac} \lesssim 1m$, it is found out that in the laboratory(Khoury and Weltman, 2004b)

$$\alpha \leq 10^{-3}. \tag{3.2.2}$$

It has been demonstrated (Khoury and Weltman, 2004b) that the Chameleon model satisfies this constraint perfectly well but with the proviso that the test bodies must have thin-shell.

Let's recap how it was demonstrated.

If a test mass of uniform density ρ_c,,radius R_c and mass M_c is assumed to have thick-shell then it will generate the field profile (2.3.2)

$$\phi \approx -\left(\frac{\beta}{4\pi}\right)\left(\frac{M_c}{M_{pl}}\right)\frac{e^{-\frac{r}{R_{vac}}}}{r} + \phi_{vac}. \tag{3.2.3}$$

The potential energy for (3.2.3) can be found as follows:

$$\nabla\phi \approx \left(\frac{\beta}{4\pi}\right)\left(\frac{M_c}{M_{pl}}\right)\left(\frac{1}{rR_{vac}} + \frac{1}{r^2}\right)e^{-\frac{r}{R_{vac}}} \tag{3.2.4}$$

Neglecting non-linear powers of r, we have,

$$\nabla\phi \approx \left(\frac{\beta}{4\pi}\right)\left(\frac{M_c}{M_{pl}}\right)\left(\frac{1}{rR_{vac}}\right)e^{-\frac{r}{R_{vac}}} \approx \left(\frac{\beta}{4\pi}\right)\left(\frac{M_c}{M_{pl}}\right)\frac{e^{-\frac{r}{R_{vac}}}}{r}. \tag{3.2.5}$$

(3.2.5) into (3.1.5) gives:

$$F_\phi \approx -\frac{M_c\beta}{M_{pl}}\nabla\phi = -\left(\frac{\beta^2}{4\pi}\right)\left(\frac{M_c^2}{M_{pl}^2}\right)\frac{e^{-\frac{r}{R_{vac}}}}{r} = -\left(\frac{2\beta^2}{8\pi}\right)\left(\frac{M_c^2}{M_{pl}^2}\right)\frac{e^{-\frac{r}{R_{vac}}}}{r} \tag{3.2.6}$$

Thus,

$$V(r) \approx F_\phi R = F_\phi R_{vac} = F = -\left(\frac{2\beta^2}{8\pi}\right)\left(\frac{M_c^2}{M_{pl}^2}\right)\frac{e^{-\frac{r}{R_{vac}}}}{r} \tag{3.2.7}$$

Comparing (3.2.1) and (3.2.7) we see that:

$$\alpha = 2\beta. \tag{3.2.8}$$

For coupling constants of order unity $\beta \sim o(1)$, $\alpha \gg 10^{-3}$. This is a clear disagreement with a laboratory observation (3.2.2).

Let's now assume that the test mass has a thin-shell. Then, it will generate the profile (2.3.1)

$$\phi \approx -\left(\frac{\beta}{4\pi M_{pl}}\right)\left(\frac{3\Delta R_c}{R_c}\right)\frac{M_c e^{-\frac{r}{R_{vac}}}}{r} + \phi_{vac}. \tag{3.2.9}$$

To find the potential energy associated with (3.2.9), we go through steps similarly to the thick-shell case:

$$\begin{aligned}\nabla\phi &\approx \left(\frac{M_c\beta}{4\pi M_{pl}}\right)\left(\frac{3\Delta R_c}{R_c}\right)\left(\frac{1}{rR_{vac}} + \frac{1}{r^2}\right)e^{-\frac{r}{R_{vac}}} \\ &= \left(\frac{M_c\beta}{4\pi M_{pl}}\right)\left(\frac{3\Delta R_c}{R_c}\right)\frac{e^{-\frac{r}{R_{vac}}}}{r}.\end{aligned} \tag{3.2.10}$$

Again,

$$F_\phi \approx -\frac{M_c\beta}{M_{pl}}\nabla\phi = -\left(\frac{\beta^2}{4\pi}\right)\left(\frac{3\Delta R_c}{R_c}\right)\left(\frac{M_c^2}{M_{pl}^2}\right)\frac{e^{-\frac{r}{R_{vac}}}}{r}.$$

So,

$$V(r) = F_\phi R = F_\phi \left(\frac{3\Delta R_c}{R_c}\right) R_{vac} = F_\phi \left(\frac{3\Delta R_c}{R_c}\right)$$
$$= -2\beta^2 \left(\frac{3\Delta R_c}{R_c}\right)^2 \left(\frac{M_c^2}{8\pi M_{pl}^2}\right) \frac{e^{-\frac{r}{R_{vac}}}}{r}. \tag{3.2.11}$$

Comparing (3.2.11) with (3.2.1) , and noting that $\frac{\Delta R_c}{R_c} \equiv \frac{\phi_{vac} - \phi_c}{6\beta M_{pl}\Phi_c} \ll 1$,we see that $2\beta \left(\frac{3\Delta R_c}{R_c}\right)^2 = \alpha \lesssim 10^{-3}$.

Indeed, as long as test masses with thin-shell are used in the vacuum chamber, the current constraints on the search for fifth force are met by Chameleon Models.

3.3 Solar System Tests

Using (2.2.46) and comparing (2.2.38) with (2.2.41), it can be easily seen that the thin-shell effect makes satisfying the constraints imposed on Chameleon Models from solar system tests trivial. In other words, since

$$\beta_{eff} = 3\beta \frac{\Delta R_\oplus}{R_\oplus} < 3\beta.10^{-7} \tag{3.3.1}$$

is so small, all solar system tests constraints are satisfied.

Also, the fields within these sufficiently large bodies are approximately constant, $\phi \sim \phi_c \rightarrow \nabla\phi = 0$. Thus, the fifth force generated by the sun or any of its planets only come from a thin-shell beneath its surface which is too tiny to have any noticeable effect on test bodies.

It has been shown Khoury and Weltman (2004b) that Chameleon models satisfy even stringent bound on violation the Equivalence Principle obtained through Lunar Laser ranging (Will, 2005).

$$\frac{|a_{moon} - a_\oplus|}{a_{moon} + a_\oplus} \approx \frac{|a_{moon} - a_\oplus|}{a_\oplus} \lesssim 10^{-13} \tag{3.3.2}$$

In the seminal and pioneering work on the Chameleon Model, (Khoury and Weltman, 2004b), the moon was shown to have a thin-shell though the following calculations:

from the thin-shell condition, we can write

$$\frac{\Delta R_{moon}}{R_{moon}} = \frac{\phi_G - \phi_{moon}}{6\beta M_{pl}\Phi_{moon}} \tag{3.3.3}$$

but we know that $\phi_G \gg \phi_{moon}$, $\phi_G \gg \phi_\oplus$ and so it is safe to write

$$\frac{\Delta R_{moon}}{R_{moon}} \approx \frac{\phi_G}{6\beta M_{pl}\Phi_{moon}}. \tag{3.3.4}$$

we can also write:

$$\frac{\triangle R_\oplus}{R_\oplus} = \frac{\phi_G - \phi_\oplus}{6\beta M_{pl}\Phi_\oplus} \approx \frac{\phi_G}{6\beta M_{pl}\Phi_\oplus} \tag{3.3.5}$$

$$\Phi_G = 6\beta M_{pl}\Phi_{\oplus}\frac{\triangle R_{\oplus}}{R_{\oplus}} \tag{3.3.6}$$

(3.3.6) into (3.3.4) leads to

$$\frac{\triangle R_{moon}}{R_{moon}} \approx \frac{6\beta M_{pl}\Phi_{\oplus}\frac{\triangle R_{\oplus}}{R_{\oplus}}}{6\beta M_{pl}\Phi_{moon}} = \frac{\triangle R_{\oplus}}{R_{\oplus}}\frac{\Phi_{\oplus}}{\Phi_{moon}}. \tag{3.3.7}$$

Using $\Phi_{\oplus} = 10^{-9}$, $\Phi_{moon} = 10^{-11}$ and $\frac{\triangle R_{\oplus}}{R_{\oplus}} < 10^{-7}$,

(3.3.7) becomes

$$\frac{\Delta R_{moon}}{R_{moon}} < 10^{-5}. \tag{3.3.8}$$

Definitely, the moon has a thin-shell.

With the knowledge that the Sun and Moon have thin-shell, it is easy to see that the Chameleon model satisfies the LLR bound:

From (3.1.8), it is not difficult to see that the acceleration of a compact object, say object i, that have thin-shell toward the sun is :

$$a_i = a_N\left[1 + 2\beta^2\left(\frac{3\triangle R_i}{R_i}\right)\left(\frac{3\triangle R_{\odot}}{R_{\odot}}\right)\right]. \tag{3.3.9}$$

Where a_N,the Newtonian acceleration, is given is

$$a_N = \frac{G_N M_{\odot}}{r^2} \tag{3.3.10}$$

and r is the separation between the Sun and compact object i.

So, for the Earth, (3.3.9) becomes

$$a_{\oplus} = a_N\left[1 + 18\beta^2\left(\frac{\triangle R_{\oplus}}{R_{\oplus}}\right)\left(\frac{\triangle R_{\odot}}{R_{\odot}}\right)\right]. \tag{3.3.11}$$

But

$$\frac{\triangle R_{\odot}}{R_{\odot}} = \frac{\phi_G - \phi_{\oplus}}{6\beta M_{pl}\Phi_{\odot}} \approx \frac{\phi_G}{6\beta M_{pl}\Phi_{\odot}} = \frac{\Delta R_{\oplus}}{R_{\oplus}}\frac{\Phi_{\oplus}}{\Phi_{\odot}}.$$

So,

$$a_{\oplus} = a_N\left[1 + 6\beta^2\left(\frac{\triangle R_{\oplus}}{R_{\oplus}}\right)^2\left(\frac{\Phi_{\oplus}}{\Phi_{\odot}}\right)\right]. \tag{3.3.12}$$

Also,

$$a_{moon} = a_N \left[1 + 2\beta^2 \left(\frac{3\Delta R_{moon}}{R_{moon}} \right) \left(\frac{3\Delta R_\odot}{R_\odot} \right) \right] \approx a_N \left[1 + 18\beta^2 \left(\frac{\Delta R_\oplus}{R_\oplus} \right)^2 \left(\frac{\Phi_\oplus^2}{\Phi_\odot \Phi_{moon}} \right) \right]. \quad (3.3.13)$$

Using the $\Phi_\odot = 10^{-6}$, $\Phi_\oplus = 10^{-9}$ and $\Phi_{moon} = 10^{-11}$, then:

$$\frac{|a_{moon} - a_{\oplus|}}{a_N} \approx \beta^2 \left(\frac{\triangle R_\oplus}{R_\oplus} \right)^2 < \beta^2 10^{-14}. \quad (3.3.14)$$

With $\beta \sim O(1)$, this clear satisfies the bound established by the LLR.

3.4 Cosmological Tests

We can use gravitational redshift to test the Equivalence Principle (actually, Local Position Invariance).

Einstein's theory of general relativity tells us that the redshift z is given by

$$z = \frac{\triangle\lambda}{\lambda} = \frac{\triangle v}{c} = \frac{a_N \triangle t}{c} = \frac{1}{c} \int \nabla\Phi_N dt = \triangle\Phi_N \quad (3.4.1)$$

(Carroll, 2004)

The violation of the Local Position Invariance can be quantified as:

$$\triangle z = \alpha \triangle\Phi \quad (3.4.2)$$

, where α is zero for Einstein's theory and it depends on the nature of the clock whose redshift is being measured.Will (2005)

The strongest constraint on the variation of coupling constant

$$|\alpha| \leq 10^{-4} \quad (3.4.3)$$

comes from the Vessot-Levine experiment. (Khoury and Weltman, 2004b)

we can write:

$$\rho(\phi) = \rho^{(i)} e^{4\frac{\beta_i \phi}{M_{Pl}}} \quad (3.4.4)$$

In natural units, $[\rho] = M^4$ and $[\nu] = M^1$.

Thus,

$$\triangle\nu = \frac{\beta_i}{M_{pl}} \nu^{(i)} e^{\frac{\beta_i \phi}{M_{Pl}}} \triangle\phi \quad (3.4.5)$$

$$\triangle z = \frac{\triangle\nu}{\nu} = \frac{\beta_i}{M_{pl}} \triangle\phi = -\frac{\beta_i}{M_{pl}} \left(\phi(r_{em}) - \phi(r_{rec}) \right)$$

The following values were used in the Vessot-Levine experiment[]: $r_{em} \approx 10^4 km \approx 2R_\oplus$ and $r_{rec} \gtrsim R_\oplus$

$$r_{em} \approx 10^4 km \approx 2R_\oplus$$

and certainly, $\phi(r_{em}) \approx \phi_G$ and $\phi(r_{rec}) \approx \phi_{atm}$ and $\Phi_\oplus = 2\triangle\Phi$

Thus,

$$\triangle z = -\frac{\beta_i}{M_{pl}}\left(\phi(r_{em}) - \phi(r_{rec})\right) = -\frac{\beta_i}{M_{pl}}(\phi_G - \phi_{atm})$$
$$= -\frac{\beta_i}{M_{pl}}\left(\frac{\triangle R_\oplus}{R_\oplus}\right)(6\beta M_{pl})(2\triangle\phi) = -12\beta^2\left(\frac{\triangle R_\oplus}{R_\oplus}\right) \lesssim \beta^2 10^{-7}\triangle\Phi \tag{3.4.6}$$

Thus, $|\alpha| = \beta^2 10^{-7} \lesssim 10^{-4}$ for β of order unity.

We can use the similarly procedure to show that the Chameleon satisfies the limit to the variation of mass since the Big Bang nucleosynthesis, BBN to now (denoted by null).

$[\rho] = M^4$ and $\rho(\phi) = \rho^{(i)} e^{4\frac{\beta_i \phi}{M_{Pl}}} \rightarrow m(\phi) = m^{(i)} e^{\frac{\beta_i \phi}{M_{Pl}}}$

Also,

$$\triangle m = \frac{\beta_i}{M_{pl}} m^{(i)} e^{\frac{\beta_i \phi}{M_{Pl}}} \triangle\phi$$

Thus,

$$\left|\frac{\triangle m}{m}\right| = \frac{\beta_i}{M_{pl}}\triangle\phi = -\frac{\beta_i}{M_{pl}}\left(\phi_0 - \phi_{BBN}\right)$$

Whether through clock comparison, geophysical observations (like Oklo Natural reactor), $^{187}R_e$ decay in meteorites, spectra in distant quasars or the Big Bang Nucleosynthesis, bounds on variation of fundamental are tiny enough to be satisfied by Chameleon models.

Constant k	Limit on $\dot{k}/k$ (yr^{-1})	Redshift
Fine structure	$< 30 \times 10^{-16}$	0
constant	$< 0.5 \times 10^{-16}$	0.15
$\alpha_{\mathrm{EM}} = e^2/\hbar c$	$< 3.4 \times 10^{-16}$	0.45
	$(6.4 \pm 1.4) \times 10^{-16}$	$0.2 - 3.7$
	$< 1.2 \times 10^{-16}$	$0.4 - 2.3$
Weak interaction	$< 1 \times 10^{-11}$	0.15
constant	$< 5 \times 10^{-12}$	10^9
$\alpha_{\mathrm{W}} = G_{\mathrm{f}} m_{\mathrm{p}}^2 c/\hbar^3$		
e-p mass ratio	$< 3 \times 10^{-15}$	$2.6 - 3.0$

Figure 3.1: bounds on the variation of fundamental constants (Will, 2005).

3.5 Predictions

The launching of the satellites STEP, GG and MICROSCOPE, which are expected to test Eotvos parameter η 10^{-18}, 10^{-17} and 10^{-15} respectively provide a golden opportunity to truly test the validity of the Chameleon model. Doing some back of the envelop calculation, the proponents of the chameleon model (Khoury and Weltman, 2004b) found out that, given the current design of SEE satellite, it would not have a thin-shell in the range,

$$10^{-15} < \frac{\triangle R_{SEE}}{R_{SEE}} < 10^{-7}.$$

Which falls well within the range of STEP.

It has also been suggested that the Chameleon can be detected in the laboratory (Upadhye et al., 2010). That, they can induce very small but observable attractive force between two metal plates differing from what is expected from the Casimir force.

The implication of this for the chameleon model is that SEE will measure a value for gravitation constant differing by an order of unity from the measurement of gravitational constant as measured on Earth. This bold and unambiguous prediction if proven right will be a watertight argument for the existence of Chameleon-like scalar fields.

4. Conclusions and Suggestions

4.1 Conclusions

In this essay, we have seen that attempts at satisfactorily explaining the acceleration of the universe called for generalizing dark energy to that of scalar fields slowly rolling down a flat potential but doing so induces an additional force of nature which is subjected to host of experimental constraints. We also saw that generalizing the dark energy to scalar fields that couple directly or indirectly to matter and yet successfully ensuring consistency with tests of gravity can be accomplished by the chameleon mechanism. That is, the chameleon becomes massive in high density regions and thus generates fifth force of short range beyond the bounds of current experiments. In the cosmos, where the density is sparse, it acquires mass that is sufficient to drive the current acceleration of the universe. Also, for a sufficiently large object, the fifth force is generated almost entirely by a thin-shell. Future satellite experiments with t test bodies without thin-shell are predicted to be able observed scalar field effects like a variation of the gravitational constant of an order of unity.

4.2 Suggestions

Given that the Chameleon itself is the offspring of of extra-dimensions to reconcile theories or make a theory agrees with empirical evidence and established facts, the very idea of extra-dimension needs much more thorough scrutiny. We should keep an open mind for the It is possibility of concept of extra-dimension being just another "epicycle".

Also, inferring the distant or early universe from nearby or today's universe, which is the primary evidence for the acceleration of the universe, when our understanding of the origin and evolution of mass and formation of galaxy is very poor is analogous to an alien making conclusions about adulthood by merely studying children without the slightest idea on the changes that occur between childhood and adulthood. Since the luminosity of a star, yea a galaxy, is a function of its mass and that the mass distribution of stars in galaxy depends on the way the galaxy was formed, I suggest that without enough information on the origin and evolution of mass and the mass distribution of stars in galaxies, conclusive statements about the acceleration of our universe can not be drawn. The idea of dark flow (Arbey, 2008)(Tsagas, 2011) is appetizing to be also be examined.

Finally, chameleon models are built on the premise that general relativity is valid on all scales but it is highly conceivable that dark matter and dark energy are the telltale signals that general relativity breaks down on the large scale. The chameleon and all attempts at patching up general relativity to work on cosmological scales might be tantamount to attempting to modify Newtonian mechanics to work on the quantum scale when what is actually needed is complete discarding of some cherished concepts and fundamental premises of classical mechanics. Moreover, the mass of the chameleon is purported to be in the neighbourhood of the Planck mass yet Chameleon models are developed with not much thought on the fact that at Planck scale quantum gravity effects must become important.

In conclusion, though Chameleon mechanism is interesting for the fact that it allows the existence of light scalars, without the violations of established empirical constraints, and that it somewhat alleviates the Cosmic coincidence problem (though it has a fine-tuning problem of its own), to make true breakthroughs in our understanding of the mysterious processes and exciting physics occurring on both the largest and smallest of scales, we need a theory of quantum gravity. If we really intend ever unravelling the deepest secret of our universe then a theory of quantum gravity is no longer a luxury but a must.

Acknowledgements

My thanks and appreciations go to the the following persons for their helps and supports. My supervisor, Dr. Amanda Weltman, for providing guidance, for critically reading through this essay and providing the necessary corrections. The African Institute for Mathematical Sciences for providing all the supports and excellent studying environment, without which this work would never have been possible. I am also grateful to all the tutors, particularly Mr. Markus Kugger, for taking special interest in my studies and for giving me needed encouragement. To all my colleagues and classmates for their friendliness, understanding and discussions that have immensely contributed to my insights in the Mathematical sciences.

References

Erich G Adelberger, Blayne R Heckel, and AE Nelson. Tests of the gravitational inverse-square law. *arXiv preprint hep-ph/0307284*, 2003.

A Arbey. Cosmological constraints on unifying dark fluid models. *arXiv preprint arXiv:0812.3122*, 2008.

Eugeny Babichev and David Langlois. Relativistic stars in f (r) and scalar-tensor theories. *Physical Review D*, 81(12):124051, 2010.

Matthias Blau. *Lecture Notes on General Relativity*. Albert Einstein Center for Fundamental Physics, 2011.

Philippe Brax, Carsten van de Bruck, David F Mota, Nelson J Nunes, and Hans A Winther. Chameleons with field-dependent couplings. *Physical Review D*, 82(8):083503, 2010.

Max Camenzind. *Compact objects in astrophysics*. Springer, 2007.

Sean M Carroll. Quintessence and the rest of the world: suppressing long-range interactions. *Physical Review Letters*, 81(15):3067–3070, 1998.

Sean M Carroll. *Spacetime and geometry. An introduction to general relativity*, volume 1. 2004.

Sean M Carroll, William H Press, Edwin L Turner, et al. The cosmological constant. *Annual Review of Astronomy and Astrophysics*, 30(1):499–542, 1992.

H Dittus and C Lämmerzahl. Experimental tests of the equivalence principle and newton's law in space. In *GRAVITATION AND COSMOLOGY: 2nd Mexican Meeting on Mathematical and Experimental Physics. AIP Conference Proceedings*, volume 758, pages 95–112, 2005.

Joshua Frieman, Michael Turner, and Dragan Huterer. Dark energy and the accelerating universe. *arXiv preprint arXiv:0803.0982*, 2008.

A Hees and A Füzfa. Combined cosmological and solar system constraints on chameleon mechanism. *Physical Review D*, 85(10):103005, 2012.

Justin Khoury and Amanda Weltman. Chameleon fields: Awaiting surprises for tests of gravity in space. *Phys. Rev. Lett.*, 93:171104, Oct 2004a. doi: 10.1103/PhysRevLett.93.171104. URL http://link.aps.org/doi/10.1103/PhysRevLett.93.171104.

Justin Khoury and Amanda Weltman. Chameleon cosmology. *Physical Review D*, 69(4):044026, 2004b.

Anna M Nobili, Gian Luca Comandi, Suresh Doravari, Donato Bramanti, Rajeev Kumar, Francesco Maccarrone, Erseo Polacco, Slava G Turyshev, Michael Shao, John Lipa, et al. "galileo galilei"(gg) a small satellite to test the equivalence principle of galileo, newton and einstein. *Experimental Astronomy*, 23(2):689–710, 2009.

Thanu Padmanabhan. Cosmological constant—the weight of the vacuum. *Physics Reports*, 380(5): 235–320, 2003.

Adam G Riess, Alexei V Filippenko, Peter Challis, Alejandro Clocchiatti, Alan Diercks, Peter M Garnavich, Ron L Gilliland, Craig J Hogan, Saurabh Jha, Robert P Kirshner, et al. Observational evidence from supernovae for an accelerating universe and a cosmological constant. *The Astronomical Journal*, 116(3):1009, 1998.

Christos G Tsagas. Peculiar motions, accelerated expansion, and the cosmological axis. *Physical Review D*, 84(6):063503, 2011.

Shinji Tsujikawa, Takashi Tamaki, and Reza Tavakol. Chameleon scalar fields in relativistic gravitational backgrounds. *Journal of Cosmology and Astroparticle Physics*, 2009(05):020, 2009.

Slava G Turyshev. Experimental tests of general relativity. *arXiv preprint arXiv:0806.1731*, 2008.

A Upadhye, JH Steffen, and A Weltman. Constraining chameleon field theories using the gammev afterglow experiments. *Physical Review D*, 81(1):015013, 2010.

Jean-Philippe Uzan. The fundamental constants and their variation: observational and theoretical status. *Reviews of modern physics*, 75(2):403, 2003.

TP Waterhouse. An introduction to chameleon gravity. *arXiv preprint astro-ph/0611816*, 2006.

Steven Weinberg. The cosmological constant probiem. *Rev. Mod. Phys*, 61(1), 1989.

Clifford M Will. The confrontation between general relativity and experiment. *arXiv preprint gr-qc/0510072*, 2005.

Ivaylo Zlatev, Limin Wang, and Paul J Steinhardt. Quintessence, cosmic coincidence, and the cosmological constant. *Physical Review Letters*, 82(5):896–899, 1999.